Hydrodynamic Changes in Sand due to Biogrowth on Naphthalene and Decane

Angela R. Bielefeldt[1]; Camille McEachern[2]; and Tissa Illangasekare[3]

Abstract: Biological activity in zones of chemical contamination changes the pore characteristics that control the flow of water and transport of dissolved chemicals in soils. To further the understanding of these processes, column experiments were performed to evaluate the effect of biomass growth on decane or naphthalene dissolved in simulated groundwater on the hydraulic conductivity and dispersivity of sand. The effect of grain size, groundwater flowrate, and nitrogen limitation were investigated. Given the low carbon loading resulting from the solubility of decane and naphthalene, sparse and discontinuous biomass growth reduced the hydraulic conductivity of the sand by 2 to 3 orders of magnitude after 35 to 63 days. This biogrowth initially increased dispersivity of the sand, but after longer periods of growth dispersivity, decreased to stable values near that of the clean sand. The results indicate that biogrowth can have significant effects in natural systems with low carbon loading and nitrogen availability, and should be taken into account when using models to predict contaminant transport in the field.

DOI: 10.1061/(ASCE)0733-9372(2002)128:1(51)

CE Database keywords: Hydrodynamics; Sand; Biofilm; Porous media; Hydraulic conductivity.

Introduction

When organic contaminants, such as jet fuels, that are in the form of nonaqueous phase liquids (NAPL's) are released into the subsurface, there are generally indigenous bacteria in the soil that have the capability to degrade these compounds as a growth substrate. Because of the low solubilities of the NAPL constituents (e.g., naphthalene, decane), the dissolved concentrations of the organics in the groundwater are generally very low. Most of the bacteria in the subsurface that potentially degrade the dissolved organics are attached to the soil grains (Rittmann 1993), but some are also suspended and transported through the subsurface. Depending on the amount of biomass growth, the bacterial accumulation may affect the groundwater flow and solute transport. Of specific interest are changes in the hydraulic conductivity of the aquifer material. The groundwater velocity, which depends on the hydraulic conductivity, affects both aquifer discharge and the rate of migration of dissolved chemicals. Because the flowing groundwater transports electron acceptors and nutrients required for the bacterial growth in addition to the contaminants, conductivity changes could significantly impact the fate of contamination in the subsurface. In addition, biomass growth that changes the pore characteristics is expected to affect dispersivity both at the micro- and macroscales, thus impacting the spread of contaminants and the concentrations of the toxicants appearing at receptor points.

A number of previous experiments have investigated biofilm growth in porous media represented by glass beads or sand. Taylor and Jaffe (1990a), Cunningham et al. (1991), and Vandevivere and Baveye (1992) all studied hydraulic conductivity changes of porous media due to biofilm growth. All of those studies used high solubility compounds that are easily biodegraded as the bacterial growth substrates (methanol and glucose). The average linear groundwater velocity due to hydraulic loading was somewhat high in some experiments, ranging from 0.06–20 cm/min. However, the effect of different groundwater velocities was not directly comparable between experiments under otherwise similar conditions. Cunningham et al. (1991) also investigated the effect of porous media size by comparing glass spheres and three different sizes of sand.

Both Taylor and Jaffe (1992c) and Sharp et al. (1999) have reported on changes in dispersivity with biofilm growth, but the effect of biofilms resulting from very low organic loading (such as the case for dissolution from entrapped NAPL sources) on dispersivity have not been reported. Dispersivity is an important parameter in models such as BIOPLUME (Rafai et al. 1998) and BIOSCREEN (Newell et al. 1996), which have been used to evaluate the efficacy of natural attenuation as a remedial alternative that provides acceptable risks to downstream receptors.

Rittmann (1993) proposed unifying concepts allowing tests under widely varying conditions to be systematically compared. The surface-loading rate of substrate (measured as COD) is used along with knowledge of biokinetic parameters to calculate a normalized surface loading (NSL). This NSL indicates whether a continuous biofilm on the surface of the soil is expected ($NSL > 1$), or whether only discontinuous biofilms can be supported ($NSL < 0.25$). It is generally difficult to fully quantify all of the parameters in the equations. However, Rittmann (1993) calculated surface loadings and normalized surface loadings for 11

[1]Assistant Professor, Dept. of Civil, Environmental, & Arch. Engineering, Univ. of Colorado, Boulder, Campus Box 428, Boulder, CO 80309-0428 (corresponding author). E-mail: bielefel@stripe.colorado.edu

[2]Senior Design Engineer, Camille Buehler Consulting, P.O. Box 1511, Susanville, CA 96130.

[3]Professor, Environmental Science and Engineering, Colorado School of Mines, Golden, CO 80401-1887.

Note. Associate Editor: Eric A. Seagren. Discussion open until June 1, 2002. Separate discussions must be submitted for individual papers. To extend the closing date by one month, a written request must be filed with the ASCE Managing Editor. The manuscript for this paper was submitted for review and possible publication on July 25, 2000; approved on July 18, 2001. This paper is part of the ***Journal of Environmental Engineering***, Vol. 128, No. 1, January 1, 2002. ©ASCE, ISSN 0733-9372/2002/1-51–59/$8.00+$.50 per page.

different experiments, which ranged from 0.01 to 130 g COD/m^2-d and 0.07 to 870, respectively.

The primary objective of the research presented in this article was to understand and quantify the effects of bioprocesses on the fate and transport behavior of low solubility organic compounds representative of petroleum fuels. These compounds dissolve slowly out of light nonaqueous phase liquids (LNAPLs), serving as long-term sources of low carbon loading into the groundwater. The effects of biodegradation of these compounds on the transport and flow parameters of sandy soils were investigated in the laboratory using packed columns. The influence of the sand grain size, groundwater flow rates, and nitrogen availability on changes in the hydraulic conductivity and dispersivity due to biomass growth were systematically studied in order to simulate a range of conditions that could be encountered in a natural aquifer. The information gained will be useful when applying mathematical models to predict and assess the environmental impacts of these chemicals on the subsurface and groundwater under conditions of bioactivity.

Materials and Methods

Clean quartz sands were used throughout the experiments to represent aquifer material. (The previously measured characteristics of the three sand sizes used are summarized in columns 1 to 4 of Table 2.) Before use the sand was passed through a No. 200 sieve to remove fines and burned at 550°C to remove organic matter.

The bacterial cultures used were enriched from near-runway soil from Denver International Airport. A 5 g aliquot of soil was added to 500 mL of simulated groundwater (SGW) containing the carbon source of interest (naphthalene crystals in a porous bag or 500 μL of decane) and incubated on a shaker table at room temperature. The simulated groundwater (SGW) contained the following compound concentrations (in mg/L) in deaerated Milli-Q purified water: 700 KH_2PO_4, 1,000 K_2HPO_4, 100 NH_4Cl, 50 $CaCl_2$, 17 $MgSO_4$, 12 NaCl, 0.6 $FeSO_4$, 0.22 $ZnSO_4$, 0.27 $MnSO_4$, 0.09 $Al_2(SO_4)_3$, 0.07 $CuSO_4$, 0.05 $Na_2B_4O_7$, 0.04 $CoCl_2$, 0.03 Na_2MoO_4, and 0.02 $NiSO_4$. After 2 weeks, the solution was centrifuged to remove the soil, and the supernatant was used to continue bacterial growth in flasks containing 500 mL of SGW. Every 3 to 4 days, 50 mL of liquid was removed from the growth flask and replaced with fresh SGW and 20 μL of decane or 20 mg naphthalene. Prior to the start of the column experiments, 200 mL of the appropriate enrichment culture (as diluted with SGW) was mixed with 490 g of sand, and then packed into the columns. The goal of precontacting the sand and bacteria was to produce an initially even spatial distribution of the bacteria throughout the sand. A sample of the seed biomass and the initial pore volume of column effluent were analyzed to determine the initial amount of biomass in the sand column.

A schematic diagram of the column set-up is shown in Fig. 1. Columns 7 cm inner diameter (i.d.)×15 cm tall were constructed of Plexiglas. A 3 cm layer of gravel (3 mm average diameter) was packed at each end of the column to provide uniform groundwater flow into the sand, which was about 8 cm deep. Simulated groundwater containing naphthalene (nap) or decane was continuously recirculated through the columns vertically upwards using a peristaltic pump set at a constant flowrate. The NH_4Cl concentration in the SGW was modified as needed to achieve the desired carbon:nitrogen (C:N) ratio. Batches of 250 mL of the SGW were changed out three times per week. In decane experiments, 157 μL of decane (Fisher Scientific, 99.2% purity) was added per batch of

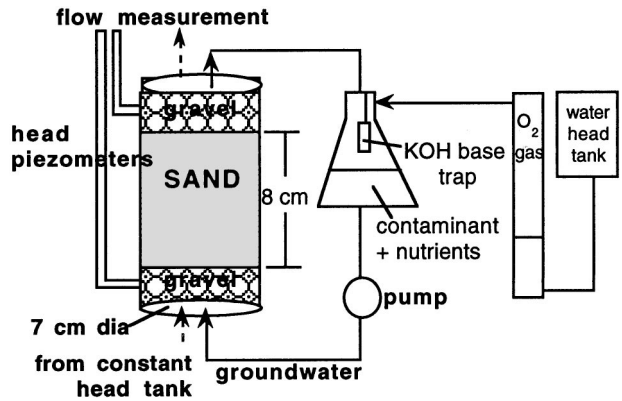

Fig. 1. Column apparatus used to measure effects of biogrowth in porous media

SGW. The decane LNAPL dissolved into solution over time. The SGW fed to the column was drawn from the bottom of the flask (assumed to be near the water solubility of 0.04 mg decane/L; 57 mg decane/day available but due to solubility limits and column flowrate likely loading near 0.7 mg decane/day). Naphthalene (Fisher Scientific, 99.98% purity) was predissolved in the SGW at 20 mg/L, giving an average loading of 2.5 mg nap/d. The SGW fed into killed controls contained no carbon source and 300 mg/L sodium azide. The 500 mL feed flasks were continuously mixed on a rotary shaker table at 160 rpm. The flasks were closed with a rubber stopper, with a 20 mL glass vial containing 10 mL of 10 N KOH attached to the bottom. This base trap sorbed biorespired carbon dioxide out of the system causing oxygen from an attached manometer to be fed into the system. This maintained aerobic conditions in the SGW. The entire setup was operated at room temperature of 20 to 25°C.

When the SGW was changed out (every 2–3 days), the ammonia, carbon chemical, and biomass concentrations were measured. Ammonia was measured by the Nessler method (APHA 1992) using Hach solutions. Carbon compound concentrations (decane or naphthalene) were measured by direct aqueous injection into a Hewlett-Packard 5890 Series II gas chromatograph with flame ionization detector (GC-FID) and a DB-5 0.32 mm i.d.×25 m capillary column. The oven temperature program was 60 °C for 2 min, followed by a 20 °C/min ramp to 200 °C where it was held for 2 min. Biomass dry weight was measured as volatile suspended solids (VSS) (APHA 1992).

The hydraulic conductivity (K) of the sand in the column was measured three times per week by treating the column as a constant head permeameter. First, the normal water flow to the column from the feed flask via the peristaltic pump was stopped. Then de-aerated water containing 20% of the normal nutrient concentrations in the SGW and no carbon source was introduced into the bottom of the column from a constant head reservoir. The head was adjusted to achieve a flowrate at or below the rate at which the SGW was normally circulated. The quantity of water leaving the top of the column over a given period of time was measured (a minimum of 2 min or 5 mL). Pressure heads before and after the sand were measured via piezometers attached to the column wall at the level of the gravel packs (the head loss in the coarser gravel pack was assumed negligible). The discharge and hydraulic head loss across the sample were used to calculate K using Darcy's Law. Three measurements at different inlet heads were made in series and averaged to represent each analysis date; these replicate K values generally varied by 0.5–10% (larger

Table 1. Summary of Experimental Conditions in Columns

Exp Number and test variable	Number of test columns	Avgerage sand size (mm)	Organic chemical in feed water and average loading	Seepage velocity[a] (cm/min)	C:N mass ratio in water	Initial seeded biomass (mg/g sand)	Days of growth before sacrifice
1—sand size	3	0.49, 0.32, 0.19	decane 0.7 mg/d	0.78	7:1	0.21	37
2—N limited	3 (1)[b]	0.32	nap 2.5 mg/d (control)	0.10	5:1, 40:1, 100:1	0.06	47, 63
3—velocity	5 (1)[b]	0.32	nap 2.5 mg/d (control)	0.52	40:1	0.09	12–44
4—velocity	6 (2)[b]	0.32	nap 2.5 mg/d (control)	0.78, 0.23	40:1	0.07	20–55

[a]Calculated from the flowrate (mL/min) using the cross-sectional area of the column and the initial porosity of the clean sand, which ranged from 0.40 to 0.46.

[b]Numbers in parentheses represent killed control columns

error associated with very small head drop). After the conductivity test, the feed solution to the columns was changed out, and the system was returned to normal recirculation flow. The entire conductivity testing plus feed changing process generally required 1 h.

Dispersivity (α) in the sand was measured using a conservative tracer test. A 2–4 mL quantity of 0.5 M KBr or 0.34 M NaCl solution was pulse injected into the inlet tubing to the column while upward groundwater flow was supplied from the constant head reservoir. Water leaving the top of the column was sampled and analyzed for tracer content using an Orion conductivity or bromide probe. Tracer breakthrough curves were analyzed using the analytical solution to the one-dimensional advection-dispersion equation (Freeze and Cherry 1979) to back-calculate the hydrodynamic dispersion, D. The solver function in Excel was used to fit tracer mass and D by minimizing the error between the measured tracer breakthrough curve and the predicted curve. This computed D was converted into dispersivity, α, by dividing by the average linear velocity, v, estimated from measured Darcy velocity and the porosity of the packed sample.

When the columns were sacrificed after the hydraulic conductivity appeared to reach steady-state, the amount of biomass attached to the sand was measured as volatile solids (VS) per dry weight of sand. Sand was cored from the column at nine locations using plastic straws with 6–10 mm diameter. Some straws were sectioned to measure differences in the biomass quantity at the top and bottom of the column. Samples of the sand were also taken for microscopic analysis. The wet sand from the core was placed on a slide and viewed using Nomarski interference at 400× magnification. The sampling procedure was not intended to maintain the packed pore structure of the sand, and the biofilms were likely to have been significantly disturbed during the slide preparation. Biofilm thickness was estimated by using a scaled reticle and viewing the edge of sand particles. The sand was sampled at nine locations, and for each sample 8–10 observations of biofilm thickness was made. The quantity of biomass attached to the gravel packs was also measured as VS per dry weight of gravel.

Periodically, the biomass suspension used to seed the sand columns was tested for naphthalene biodegradation kinetics using a batch respirometric technique (Bielefeldt and Stensel 1999b). The bacterial suspension was added into preaerated SGW in a 50 mL flask with a side-arm and septa. A Yellow Springs Instruments dissolved oxygen (DO) probe was inserted into the flask, and a gas-tight seal made. The flask now contained no headspace and was mixed with a magnetic stir bar. The DO concentration in the system was measured over time to establish the baseline endogenous oxygen uptake rate, and then an aqueous naphthalene solution was injected into the flask via the side-arm (giving 1–3 mg nap/L and non-nitrogen limited conditions). The change in DO over time was measured until the depletion rate returned to the endogenous condition. These data were then analyzed to compute the Monod biokinetic coefficients (as described in Bielefeldt and Stensel 1999b). Measured biokinetic data (maximum specific substrate degradation rate, k; half-saturation concentration, K_s; yield, Y; and endogenous decay rate, b) were used to compute normalized surface loading as discussed by Rittmann (1993) and described in Heath et al. (1990). Similar kinetic measurements for decane degradation were not possible due to its low aqueous solubility and detection limits of the DO method and gas chromatography.

Results and Discussion

The data from the column experiments were analyzed to determine the effects of biological growth at a low loading of decane and naphthalene on the hydraulic conductivity and dispersivity of sand. Variables tested included the sand size (#30, #50, and #70), nutrient limitation (C:N mass ratios approx. 5:1, 40:1, 100:1), and the water flowrate (1.5, 3.5, 8, and 12 mL/min). The measured naphthalene biodegradation kinetics of the culture were used to compute normalized surface loading. This allows comparison to a range of other experiments in packed beds and porous media. The experimental conditions during the column experiments are summarized in Table 1.

Effect of Grain Size on Biomass Growth and Hydraulic Conductivity

The decane experiment illustrated the effect of different sand grain sizes on how biomass growth affects the hydraulic properties of the saturated sand. The reported and measured characteristics of the three sands used are summarized in Table 2.

Changes in the measured hydraulic conductivity of the sand due to bacterial growth on decane at a flowrate of 12 mL/min and C:N ratio of 7:1 are shown in Fig. 2. K values measured at day 5 were similar for #30 and #50 sand, and one order of magnitude lower for #70 sand. In spite of the appearance of a lag in the conductivity decrease in the #30 and #50 sands, the day 5 conductivity values are significantly lower than reported and measured values for the clean sands (shown on the left axis in Fig. 2). The initial biomass seeded into the columns of 0.2 mg VS/g sand could have caused this observed drop in conductivity by plugging small pore throats, even if poorly attached to the sand surfaces and prior to the formation of developed biofilms (as shown in the work of Vandevivere and Baveye 1992).

After 33 days of growth, the conductivity in all sands had dropped to 7×10^{-5}–4×10^{-4} cm/s and appeared to be reaching steady state. This steady state occurs when the biomass detach-

Table 2. Hydraulic Conductivity and Dispersivity Characteristics of Different Sands Before and After Growth of Decane-Degrading Bacteria

Sand type	Reported sand characteristics[a] d_{50} (mm)	$\frac{d_{60}}{d_{10}}$	K (cm/s)	K of clean sand (cm/s)	Day 5 K (cm/s)	Avg final K (cm/s)	α of clean sand (cm)
#30	0.49	1.50	0.15	0.05	0.0249	$5.5\times10^{-4}\pm1.9\times10^{-4}$	0.044
#50	0.32	1.94	0.037	0.035	0.0125	$1.1\times10^{-4}\pm0.3\times10^{-4}$	0.027
#70	0.19	1.86	0.014	0.0049	0.0015	$1.8\times10^{-4}\pm1.0\times10^{-4}$	0.047

[a]See Illangasekare et al. (1995) and (Barth 1999).

ment due to liquid shear stress and loss due to endogenous decay are balanced by the growth on decane, resulting in apparently similar porosity available for water flow in all three columns. Between 5 and 30 days of growth, this represents two orders of magnitude decrease in the conductivity of the #50 and #30 sand and one order of magnitude decrease in the #70 sand.

After 38 days of decane feeding, the columns were sacrificed for analysis of biomass distribution. The average final volatile solids concentration on the sand was 1.45 ± 0.35, 1.20 ± 0.26, and 0.94 ± 0.34 mg VS/g sand in the #30, #50, and #70 sands, respectively. Thus, the larger grain sizes had more attached biomass. This accounts for the similar final conductivity values in all three sands because there was more biomass clogging the pores in the larger grain sand. There was not a statistically significant difference (at 90% confidence level in t test) in the amount of biomass at the bottom, middle, and top of the columns. However, there was slightly higher biomass measured at the bottom of the #50 and #70 columns (1.1 ± 0.2, 1.1 ± 0.1, 1.3 ± 0.5 mg VS/g sand top, middle, and bottom #50, respectively; 0.7 ± 0.3, 1.2 ± 0.1, 1.3 ± 0.4 mg/g sand top, middle, and bottom #70, respectively).

When sand grains from the columns were viewed under a microscope, a large variability in the biofilm thickness was evident on the individual sand grains at the microscale. Some areas contained thick clumps of biomass while other areas were virtually free of biomass. The average observed biofilm thicknesses in the #30, #50, and #70 sand were 7.5 ± 4.2, 8.6 ± 4.4, and 5.8 ± 3.1 μm, respectively. Cunningham et al. (1991) also observed that more biomass grew in columns packed with larger size media, with 10 μm biofilm thickness on 0.12 mm diameter glass beads versus 37 μm biofilm thickness on 0.5 mm sand or glass beads.

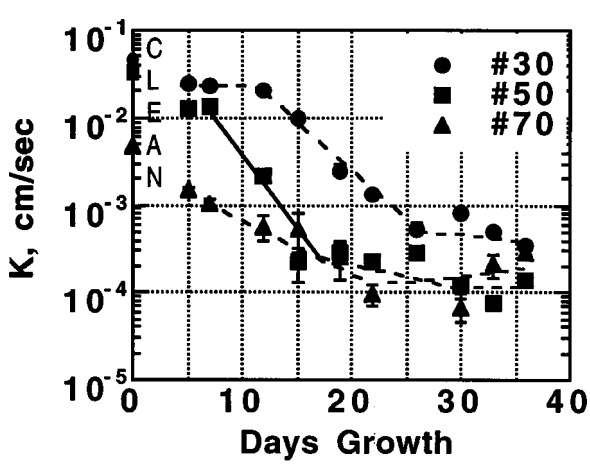

Fig. 2. Measured conductivity of uniform sand seeded with biomass and fed decane at 12 mL/min (error bars represent standard deviation of measured conductivity values)

Naphthalene Biodegradation Kinetics and Calculated Normalized Surface Loading

The measured naphthalene biodegradation kinetics of the suspended enrichment culture were: k0.60–0.64 g nap/g VSS d, K_s0.18–0.20 mg/L, Y0.62–0.65 g cell COD/g nap COD, and b0.2–0.3d^{-1}. This compares to previously reported naphthalene biokinetics of $K_s=0.09-0.21$ mg/L and $k=0.09-4$ g/g d, with cultures enriched on naphthalene having the higher k values of 0.84 to 4 g/g d (Bielefeldt and Stensel 1999a).

Flow tests were conducted to measure the effluent concentrations of naphthalene after one pass through the column. Assuming that the biodegradation rate of naphthalene was constant in the column (because the naphthalene concentration was significantly higher than K_s throughout the column), calculated values of k were 0.11 g nap/g VS d (40:1 C:N ratio and 6 mL/min flowrate) and 0.18 g nap/g VS d (100:1 C:N ratio and 3 mL/min flowrate). These values are 17–30% of the k values measured for the suspended culture. These data illustrate that care must be exercised in applying suspended growth biokinetics to biofilm systems to ensure that all appropriate factors are considered (e.g., mass transfer, nitrogen limitation, and oxygen limitation).

The normalized surface loading was calculated from the measured suspended culture biokinetics using the method of Heath et al. (1990). The estimated surface loading, J_L, was on the order of 0.001 kg COD per 1,000 m^2/d (0.0001 mg/cm^2 d), and the NSL was 0.015 at steady state for all naphthalene tests. The greatest uncertainties in these calculations were the specific surface area of the biofilm and the substrate diffusion into the biofilm, because the biokinetics including endogenous decay rate and biomass detachment were directly measured. These NSL values are in the low load regime identified by Rittmann (1993) as being associated with patchy or sparse biofilms, which is consistent with the microscopic observations made in this study. This loading regime is probably more representative of conditions present in the natural subsurface when contaminated by low solubility NAPLs such as coal tar or jet fuel, than the loadings used in similar previous studies [as summarized by Rittmann (1993) and including more recent reports by Sharp et al. (1999)].

Nutrient Limitation Effects on Biomass Growth and Hydraulic Conductivity

C:N ratios of 5:1, 40:1, and 100:1 were compared by feeding naphthalene-contaminated groundwater at 1.5 mL/min into #50 sand-packed columns. Changes in the hydraulic conductivity of

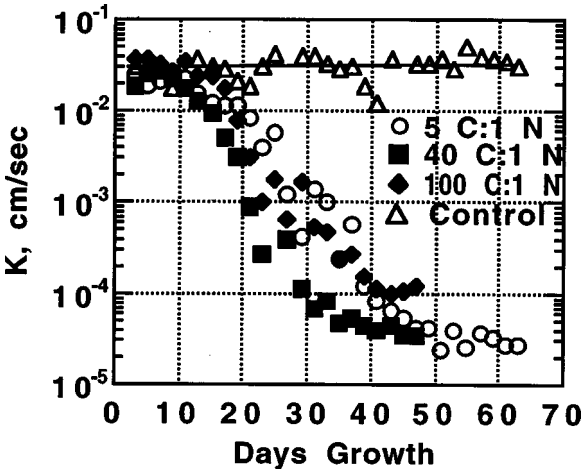

Fig. 3. Change in hydraulic conductivity of #50 sand due to biogrowth on naphthalene at 1.5 mL/min with different C:N ratios

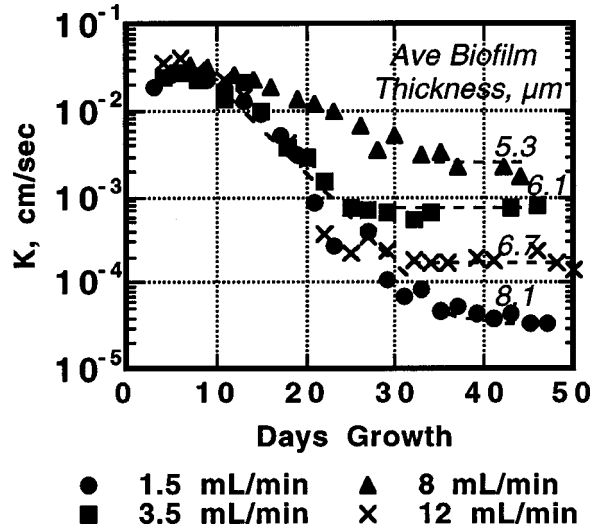

Fig. 4. Change in hydraulic conductivity of #50 sand over time due to growth on naphthalene at four different flowrates with C:N = 40:1

the sand over time are shown in Fig. 3. Over the first 12 days the hydraulic conductivity did not change significantly, but then decreased by 2–3 orders of magnitude over the next 30–40 days. The results under steady-state conditions are summarized in Table 3. Growth periods of 40–60 days were needed until steady-state hydraulic conductivity values were attained. The most nitrogen-limited condition resulted in the highest steady-state conductivity. This indicates less plugging of the sand with less nitrogen available. Lower cell yields are common for nitrogen-limited growth conditions (Gaudy and Gaudy 1980).

The biomass associated with the sand measured when the columns were sacrificed supported the conclusion of less plugging with less nitrogen available. The average measured biomass in the 100:1 and 40:1 C:N ratio columns were similar at about 0.7 mg VS/g sand and significantly less than that in the 1:5 C:N column with 1.1 mg VS/g sand. There were no trends in biomass quantity with column depth.

Effluent ammonia-N concentrations indicated that nitrogen concentrations were not severely limited in any of the columns prior to day 23, with effluent concentrations of approximately 2, 3, and 8 mg/L as N in the 100:1, 40:1, and 5:1 columns, respectively. These concentrations dropped to an average of 0.76 $\pm$0.06 mg/L past day 37 in the 100:1 column, 0.73$\pm$0.09 mg/L past day 27 in the 40:1 column, and 0.77$\pm$0.08 mg/L past day 37 in the 5:1 column. Effluent biomass concentrations from the columns during the course of the experiments were not significantly different.

Effect of Groundwater Flow Velocity

Column tests with an average naphthalene loading of 2.3 mg/d and 40:1 C:N ratio were conducted at four flowrates: 1.5 (discussed in detail above), 3.5, 8, and 12 mL/min. The estimated shear stresses for these conditions were 0.041, 0.093, 0.21, and 0.32 dyn/cm^2, respectively, as estimated using equations representing fixed beds of spherical media from Perry and Chilton (1973) as applied by Rittmann (1982). Results of the average measured hydraulic conductivity of replicate columns versus time are shown in Fig. 4. There is a lag of about 9 days in all columns before significant decreases in hydraulic conductivity are measured. For the 8, 3.5, and 1.5 mL/min flowrates there is a trend to lower final hydraulic conductivity with lower flowrate; the exception is the 12 mL/min test. Table 3 summarizes the average final "steady state" characteristics measured for the columns at the various flowrates.

The biomass corresponding to the steady-state conductivity values indicate that there is not a direct relationship between biomass and conductivity. The biomass from the 1.5 and 12 mL/min flowrates (0.69$\pm$0.08 and 0.76$\pm$0.05 mg/g, respectively) are not significantly different, although the lower flowrate had a significantly lower final conductivity (3.5×10^{-5} versus 1.8×10^{-4} cm/s, respectively). Also, the 3.5 mL/min flowrate has the

Table 3. Steady-State Characteristics of #50 Sand Containing Biomass After Naphthalene Feeding at Different Flowrates and Nitrogen Availability

C:N ratio in feed	Flowrate (mL/min)	Seepage velocity[a] (cm/min)	Days growth at "steady state"	Avg $K\pm$std dev (cm/s)	α (cm)	Avg effluent biomass $\pm$std dev (mg VSS/L)	Avg biomass$\pm$std dev (mg VS/g sand)	Avg biofilm thickness $\pm$std dev (μm)
100:1	1.5	0.10	41–47	$1.1\times10^{-4}\pm0.1\times10^{-4}$	NM[b]	4.8$\pm$2.0	0.75$\pm$0.11	9.0$\pm$5.4
40:1	1.5	0.10	45–47	$3.5\times10^{-5}\pm0.1\times10^{-5}$	NM	4.2$\pm$3.1	0.69$\pm$0.08	8.1$\pm$6.6
5:1	1.5	0.10	51–63	$3.1\times10^{-5}\pm0.6\times10^{-5}$	NM	2.5$\pm$2.4	1.10$\pm$0.22	NM
40:1	3.5	0.23	25–46	$7.0\times10^{-4}\pm0.9\times10^{-4}$	0.05	1.5$\pm$0.6	0.51$\pm$0.14	6.1$\pm$1.6
40:1	8	0.52	37–44	$2.1\times10^{-3}\pm0.3\times10^{-3}$	0.08, 0.13	2.1$\pm$1.1	0.61$\pm$0.01	5.3$\pm$2.1
40:1	12	0.78	32–50	$1.8\times10^{-4}\pm0.3\times10^{-4}$	0.06	3.8$\pm$3.5	0.76$\pm$0.05	6.7$\pm$2.3

[a]Seepage velocity approximated from Q, A, and initial porosity

[b]NM=not measured

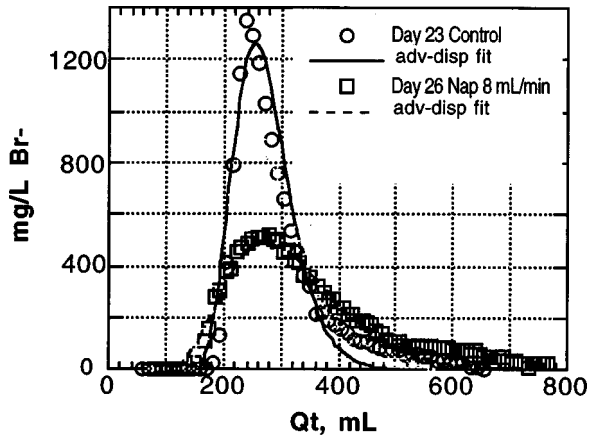

Fig. 5. Example of bromide breakthrough curves showing both data and curve fit calculated from advection-dispersion equation (flowrates were 10 and 6.5 mL/min for control and nap-fed column, respectively, $\alpha = 0.062$ and 0.20 cm for control and 26 day, respectively)

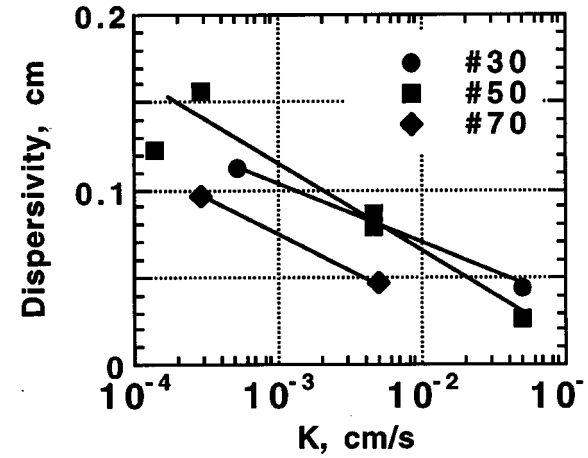

Fig. 6. Relationship between dispersivity and hydraulic conductivity in different sands containing biomass grown on decane at 12 mL/min for 12–38 days

lowest biomass but not the highest conductivity. It is likely that different biofilm structure within the porous media under the different conditions invalidates a simple correlation between the mass of bacteria in the sand and the hydraulic conductivity. The flowrate can affect the structure of the biofilms, such as higher turbulence resulting in a more dense biofilm (Characklis and Marshall 1990). The combination of flowrate and biomass data may explain the observed minimum hydraulic conductivities reached in each column. The 12 mL/min flowrate would be expected to have the highest conductivity if following the trends of the other three flowrates. But, the final measured biomass was significantly greater in the 12 mL/min column than at 3.5 and 8 mL/min, which correlates with the lower conductivity in the 12 mL/min column. Beyond the explanation that a higher shear stress gave a more dense biofilm in the 12 mL/min column, the greater availability of oxygen due to the higher recirculation rate may also have contributed to more biomass. Thus, a complex interrelationship between the flowrate, biofilm growth conditions, biofilm structure, and resulting conductivity is implied.

As shown in Fig. 4, there appears to be a correlation with thicker biofilms and the lower conductivity. However, due to the large deviation in the observed biofilm thicknesses, this is only a preliminary observation. Effluent ammonia-N concentrations from the columns were similar under all flowrates, averaging 0.63–0.95 mg/L. As shown in Table 3, effluent biomass concentrations during the period of steady-state hydraulic conductivity were similar from all columns.

Dispersivity and Porosity Changes Due to Biogrowth

Nonreactive (or conservative) tracer tests were used to calculate dispersivity in the columns, with chloride used during the decane experiments and bromide used during the naphthalene experiments. Representative tracer curves are shown in Fig. 5. The flowrate during the tracer tests varied according to the feed rate and hydraulic conductivity of the column, so the effluent concentrations are plotted against effluent volume (Qt). The lines represent the best breakthrough curve fit to the advection-dispersion equation, which was used to calculate dispersivity. There was generally more tailing to the data than predicted by the idealized breakthrough curve. This tailing likely led to the incomplete mass recovery observed, as concentrations dropped below the sensitivity of the analytic probe. Mass recovery in clean control columns ranged from 95 to 100%, compared to 70 to 100% recovery from tests in columns containing biomass (curves with less than 50% recovery were rejected due to presumed experimental errors). Similar results of incomplete tracer recovery were reported by Taylor and Jaffe (1990c), and hypothesized to be a result of diffusion of bromide into biofilms and association of bromide with bacterial extracellular polysaccharide material.

In the decane experiments, dispersivity values increased with time of biogrowth, as reflected by the lower hydraulic conductivity of the sand as shown in Fig. 6. The high conductivity values and corresponding dispersivity points were measured for the clean sand, while the lower conductivity values with higher dispersivity resulted after 12–38 days of biogrowth in the columns.

Significantly different dispersion trends were observed in the columns fed naphthalene at a high flowrate (8 and 12 mL/min), with the results shown in Fig. 7. For comparison to the biomass-affected dispersivity and K values, the large gray square in the lower right corner of the graph represents the range of dispersivity and hydraulic conductivity values measured in clean #50 sand. There is a trend to decreased dispersivity at the lower K after 19 days or more of biogrowth at 8 mL/min flowrate and more than 14 days of growth at 12 mL/min flowrate (all data points less than $K = 0.02$ cm/s). The trendline shown is the best-fit line for the 8 mL/min data beyond 19 days, which had r^2 of 0.6. As indicated by the labels on the graph, the data points resulting from short periods of biogrowth in the columns (less than 12 days) show significant deviance from the general trend in the other data. This could be due to differences in the structure of the young, not fully developed biofilms versus the older biofilms.

To test this hypothesis, data from all of the naphthalene experiments at a 40:1 C:N ratio are plotted as measured dispersivity versus time of biomass growth in the columns in Fig. 8. These data show a trend to initially increasing dispersivity, which then decreases after 15–25 days. The exception is the 3.5 mL/min test for which no dispersivity values were available before day 20, and no increase then decrease in dispersivity is evident. The dispersivity values appear to stabilize after long periods of growth (greater than 20 days minimum), but at levels somewhat higher than the dispersivity of the clean sand.

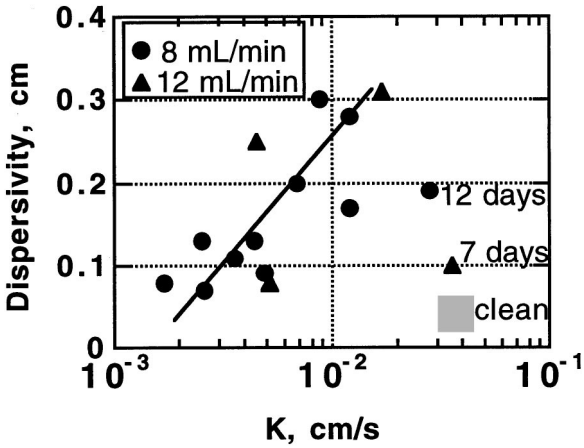

Fig. 7. Relationship between dispersivity and hydraulic conductivity of #50 sand containing biomass grown on naphthalene at 8 and 12 mL/min with C:N=40:1 for 7–50 days

The dispersivity results observed in this work are unique. Taylor and Jaffe (1990c) reported dispersivity values in bioactive columns that were 100–1000 times the values in clean sand. With a model they predicted that the dispersivity should increase predictably with increased biofilm thickness; however, their experimental data did not agree well with model-predicted values (for a given measured biofilm thickness the measured dispersivity values were 2–11 times greater than predicted by the model). They attribute this difference to the erroneous assumption of uniform biofilm thickness. However, using models they further purport that in porous media containing significant biofilm growth that transport will be dispersion dominated (due to the large dispersivity values of the biomass-containing porous media). Sharp et al. (1999) reported dispersivity increases in a system containing glass beads of 35–288% due to the presence of thick biofilms of *Pseudomonas aeruginosa*. Dispersivity increases observed in this work were up to one order of magnitude greater than in the clean system, significantly less severe than observed by Taylor and Jaffe (1990c) and in the range of those observed by Sharp et al. (1999).

The initial increases followed by decreases in dispersivity observed in this work in the naphthalene tests may be due to the low loading of the experiments (0.001 g COD/m^2*d*), which resulted in a discontinuous biofilm. If this sparse biomass accumulated at pore throats, significant differences in groundwater flow paths through the sand could result, thereby increasing dispersivity. Once more throats are clogged over longer time periods, the relative differences in pore conductivity would diminish, thereby decreasing dispersivity. By comparison, the experiments of Taylor and Jaffe (1990a) and Sharp et al. (1999) were conducted at higher surface loading rates. The approximate surface loading in the decane experiments was as high as 0.035 g COD/m^2 *d* which is near the range used in the Taylor and Jaffe work of 0.013–0.031 g COD/m^2 *d* [as reported by Rittmann (1993)]. This may be why only increasing dispersivity trends were observed in the decane experiments. Further, Torbati et al. (1986) reported that biomass preferentially filled large pore spaces in sandstone, resulting in a more homogeneous distribution of pore sizes. This increase in uniformity as the biofilms developed may have caused the observed decreases in dispersivity.

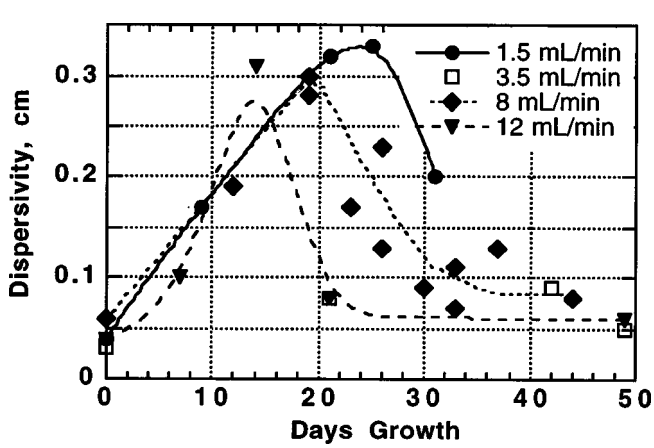

Fig. 8. Trends of dispersivity over time of biogrowth on naphthalene in #50 sand columns at different flowrates

Earlier studies on dispersivity in clean porous media have postulated that dispersivity is proportional to the average grain size of the media, and will also vary as a function of grain shape and uniformity. If the biofilm increases the effective grain size, the dispersivity should increase with increased biomass. However, the effect of biomass on the size and shape of the grains may either make them more or less regular, depending on the biofilm structure. Harleman et al. (1963) found that $D=\psi v^n d_{50}^n$, with $n=1.2$ (independent of particle shape and size, but n approaching 1 as the media becomes more nonuniform) and $\psi=0.66$ for spheres and 0.9 for angular particles. With $D=\alpha v$, this was reduced to: $\alpha=\psi v^{0.2} d_{50}^{1.2}$. Predicting the amount of dispersivity increase from this equation based on an increase in particle diameter from 0.32 mm (#50 sand) to 0.34 mm (assuming a 10 μm biofilm) would increase the dispersivity by only 8%. If the ψ increased from 0.66 for clean sand to 0.9 for sand with biomass, the dispersivity would increase by 36%. These predicted increases in dispersivity are in the range of the final dispersivity values in the steady-state naphthalene-fed columns (shown in Fig. 8) but much less than was observed during shorter periods of biomass growth on naphthalene or in the decane experiments. Therefore, the simple model predicting dispersivity on the basis of porous media characteristics does not sufficiently account for dispersivity increases due to biomass growth.

Harleman et al. (1963) also proposed a relationship between dispersivity and intrinsic permeability that can be reduced to: $\alpha=\theta v^{0.2} k^{0.6}$. Based on this equation, if K is decreased by 1–2 orders of magnitude then dispersivity should decrease by a factor of 4–16 (if the media becomes nonuniform with biomass growth then $\alpha=\phi k^{0.5}$, so a factor of 3–10). The variety of factors changing in the porous media due to biogrowth may indicate why the trends in dispersivity versus conductivity vary, depending on the predominance of the media (sand plus biomass) size, shape, irregularity, and conductivity.

In the absence of retardation of the tracer, changes in the porosity of the columns due to biomass growth could be computed from the breakthrough curves. The center of mass of these curves will occur after 1 pore volume of water has passed through the column. Because the effective pore volume of the media is reduced by the presence of biomass, the center of mass of the tracer breakthrough curve with respect to Qt should indicate the effective pore volume of the column in the presence of biomass. However, retardation of the bromide tracer is also possible, as reported by Taylor and Jaffe (1990c) who estimated retardation factors for bromide tracer of 1.3–4.7 in sand columns containing biomass. They hypothesized that this retardation occurred due to tracer

diffusion into the biofilm and/or adsorption onto exopolysaccharides in the biofilm. This combination of changes in porosity and tracer sorption are not easily separated. Calculated retardation factors in the nap experiments ranged from 1–1.4. Because the nap-fed columns contained significantly less biomass than the Taylor and Jaffe (1990c) work, smaller retardation values are logical. Estimates of porosity changes were calculated based on final measured biomass (VS converted to wet weight and then volume using an estimated biofilm density of 1.02 g/mL), and were determined to be only a 3–8% reduction from the initial porosity of the #50 sand (0.415 average). Using these porosity changes, traditional relationships such as the Kozeny-Carman equation vastly underpredicts the change in hydraulic conductivity (18% reduction due to porosity changes instead of the 99.9% reduction experimentally measured).

Comparison of Observed Results to Literature

The hydraulic conductivity changes of the sand observed over time in this study have been attributed to biomass growth, although there is the possibility that mineral precipitation as observed by Cooke et al. (1999) in anaerobic biofilms may have also contributed to plugging of the sand. Inorganic precipitation is assumed to be negligible in these experiments based on the following observations. As shown in Fig. 3, the hydraulic conductivity in killed controls did not decrease significantly over time, as would occur due to inorganic precipitates. Effluent from the columns did not contain a significantly higher TSS:VSS ratio as compared to what would be expected for biomass alone (indicating a lack of significant filterable inorganic solids). In addition, the filtrate (liquid that passed through the glass fiber filter paper) was generally clear rather that cloudy as caused by inorganic precipitates.

Due to variability in the response of the individual columns, it is difficult to derive quantitative relationships between the biomass growth and changes in the hydraulic conductivity and dispersivity. The decreases in hydraulic conductivity observed in these experiments agree fairly well with the results of Vandevivere and Baveye (1992) who observed a decrease in K of 2 orders of magnitude in 22 days in tests with 20 mg/L glucose, 0.1 mm diameter sand, 0.5 cm/min flowrate, and aerobic bacteria. The concentrations of biomass at which significant changes in the hydraulic conductivity of sand are noted vary significantly between researchers. Vandevivere and Baveye (1992) reported that less than 4 mg wet weight of biomass/mL sand did not significantly reduce K (estimated to be about 1 mg VS/mL assuming 70% water content of cells and 0.8 g VS per g dry weight; or 0.32 mg VS/mL assuming 90% water content; or 1×10^9 cells/mL). However, 10, 20, and 35 mg wet biomass/mL sand (estimated as 2.4, 4.8, and 8.4 mg VS/mL if 70% water content or 0.8, 1.6, 2.8 mg VS/mL if 90% water content) decreased conductivity by 1, 2, and 3 orders of magnitude, respectively. These biomass quantities filled 2.4, 4.8, and 8.5 percent of the available pore volume in the sand, respectively. The threshold biomass concentration with negligible conductivity effect in our experiments was approximately 0.2 mg VS/g sand, equivalent to 0.3 mg VS/mL sand; significant conductivity changes of 1–3 orders of magnitude occurred with biomass concentrations of 0.5–1.2 mg VS/g sand (0.8–1.8 mg VS/mL sand) but not in a predictable biomass: conductivity pattern. The biomass concentrations in these tests are similar to the Vandevivere and Baveye (1992) values if a 90% water content of cells is assumed (however, Vandevivere and Baveye assumed 70% water content in their calculations).

Similar to the microscopic observations of Vandevivere and Baveye (1992), it was observed that the naphthalene-degrading bacteria colonized the surface of the sand grains irregularly. Due to the disturbance of the pore structure during sampling, it is not possible to determine if assemblages of the cells were merely trapped at pore constrictions as reported by Vandevivere and Baveye; however, large clumps of cells were visible. This sparse biofilm is consistent with the NSL values per Rittman. (1993). In contrast, Cunningham et al. (1991) reported uniform biofilm thickness on glass spheres and sand media within 2–3 days of inoculation, followed by preferential biofilm accumulation on the ''down-stream'' side of the media. Both Cunningham et al. (1991) and Taylor and Jaffe (1990b) advocate that a model based on biofilm accumulation on the surfaces of the porous media which fill the pore space can be used to predict plugging of porous media. Their experimental studies were conducted with high surface loadings which should generate continuous biofilms. However, based on the observations in this work where simple relationships between biomass quantity and conductivity did not apply, the ''clogging'' model proposed by Vandevivere and Baveye (1992) seems more representative of these experiments than the ''biofilm'' model of Taylor and Jaffe (1990b). A complex interaction of both pore constriction clogging and surface biofilms likely accounts for the observed effects of biogrowth on the conductivity and dispersivity of the saturated sand.

Implications

The influence of changes in subsurface hydraulic conductivity and dispersivity due to biomass growth on the fate of toxic chemicals can be estimated using models such as BIOSCREEN (Newell et al. 1996) or MT3D. Generally, these models do not incorporate changes in the media properties due to biogrowth on the predicted fate of chemicals. Therefore, characteristics input into the model may neglect biologically-related changes in the hydraulic characteristics of the aquifer material. This will be particularly important when enhanced in -situ bioremediation is conducted, such as by adding oxygen or nitrate as electron acceptors into the subsurface to increase microbial activity.

The effect of decreased hydraulic conductivity overwhelms the fairly small decrease in porosity caused by biofilm growth, so that the pore velocity will decrease substantially (assuming that the hydraulic gradient remains the same). This slower pore velocity should increase the biodegradation, because there is a longer contact time between the bacteria and the contaminant. Using the base default parameters in BIOSCREEN and then decreasing the conductivity by 1 order of magnitude and porosity by 5%, the difference in the predicted ''centerline'' concentrations from the no degradation model versus the first-order degradation model can be compared. Where the base model predicted that with first-order biodegradation the concentration 145 ft down gradient of the source was 51% of the no biodegradation case, with the decreased conductivity and porosity the concentration predicted by the first-order model is only 2% of the no degradation model. Dispersivity changes have a somewhat less dramatic effect;increasing the dispersivity by a factor of two decreased concentrations 145 ft downgradient by 12 and 7% with no degradation and first-order biodegradation compared to the base case. All modeling exercises indicated that significant errors could be introduced by using clean sand hydrodynamic properties to approximate conditions with bioactivity in the subsurface, specifically in the zones where the NAPL phase resides.

Summary and Conclusions

Understanding and quantifying the effects of bioactivity on the flow and transport parameters becomes critical when designing effective remediation schemes at NAPL contaminated sites. Flow and transport parameters in the bioactive zones (spill zone and biobarriers) control the delivery efficiency of electron acceptors as well as the spreading of the solute plume. As a first step in understanding and quantifying the effects of biomass growth on flow and transport parameters of aquifer soils, a study was conducted using decane and naphthalene. Previous studies by other investigators tested conditions that are not representative of NAPLs with very low solubility. The results of this study show that natural soil bacteria degrading low concentrations of decane or naphthalene can significantly affect the hydraulic conductivity and dispersivity of saturated sand. The clogging of the pore spaces with biomass can decrease the hydraulic conductivity by 1–3 orders of magnitude. Due to the balancing of shear stress with biogrowth and endogenous decay, the steady-state conductivity of three different sizes of sands containing biomass were similar. Nitrogen-limitation during growth will decrease the amount of plugging of the media (higher steady-state conductivity) that is observed. There is a complex effect of biomass on the dispersivity of saturated sand. At a high flowrate and long-term growth on decane, dispersivity increased 2–5 times. With biomass grown on naphthalene at very low surface loading and NSL values, a significantly different trend was observed. For ''young'' biofilms (less than 14 days of growth) the dispersivity increased from 0.03–0.06 to 0.3–0.35 cm, and was significantly higher than the clean sand even before the hydraulic conductivity was significantly affected. After 15–25 days, the dispersivity then decreased with decreasing conductivity to near the clean sand dispersivity value. This dispersivity value was then stable. These results indicate that biomass growth in saturated soil may have a significant impact on the groundwater flow and contaminant transport beyond that due solely to the biodegradation of the contaminant. These effects should be taken into account when implementing models to predict the benefits of enhanced in-situ bioremediation.

Acknowledgments

Funding for this work was provided by the U.S. Air Force through the Great Plains/Rocky Mountain Hazardous Substance Research Center at kansas State University. The writers appreciate the assistance of Rosanna LaPlante and Samantha Illangasekare in conducting the laboratory experiments.

Notation

The following symbols are used in this paper:

D = hydrodynamic dispersion;
d_{50} = mean diameter of porous media grains, cm;
K = hydraulic conductivity;
K_s = biokinetic half-saturation concentration, mg/L;
k = intrinsic permeability;
k = biokinetic maximum specific substrate degradation rate, g/g-d;
nap = naphthalene;
α = dispersivity, cm;
ν = seepage velocity;
ψ = dimensionless coefficient based on particle shape and size distribution; and
ϕ = dimensionless coefficient based on particle shape and size distribution.

References

APHA, AWWA, and WPCF. (1992). ''Standard methods for the examination of water and wastewater.'' 18th Ed., Washington, D.C.

Barth, G. R. (1999). ''Intermediate-scale tracer tests in heterogeneous porous media: Investigation of density, predictability and characterization of NAPL entrapment.'' PhD dissertation, Univ. of Colorado, Boulder, Colo.

Bielefeldt, A. R., and Stensel, H. D. (1999a). ''Biodegradation of aromatic compounds and TCE by a filamentous bacteria-dominated consortium.'' *Biodegradation*, 10(1), 1–13.

Bielefeldt, A. R., and Stensel, H. D. (1999b), ''Evaluation of biodegradation kinetic testing methods and longterm variability in biokinetics for BTEX metabolism.'' *Water Res.*, 33(3), 733–740.

Characklis, W. G., and Marshall, K. C., eds. (1990). *Biofilms*, Wiley, New York.

Cooke, A. J., Rowe, R. K., Rittmann, B. E., and Fleming, I. R. (1999). ''Modeling biochemically drive mineral precipitation in anaerobic biofilms.'' *Water Sci. Technol.*, 39(7), 57–64.

Cunningham, A. B., Characklis, W. G., Abedeen, F., and Crawford, D. (1991). ''Influence of biofilm accumulation on porous media hydrodynamics.'' *Environ. Sci. Technol.*, 25(7), 1305–1310.

Freeze, R.A., and Cherry, J.A. (1979). *Groudwater*, Prentice-Hall, Englewood Cliffs, N.J.

Gaudy, A. F., and Gaudy, E. T. (1980). *Microbiology for environmental scientists and engineers*, McGraw-Hill, New York.

Harleman, D. R. F., Mehlhorn, P. F., and Rumer, R. R. (1963). ''Dispersion-permeability correlation in porous media.'' *J. Hydraul. Div., Am. Soc. Civ. Eng.*, 89(HY2), 67–85.

Heath, M. S., Wirtel, S. A., and Rittmann, B. E. (1990). ''Simplified design of biofilm processes using normalized loading curves.'' *Res. J. Water Pollut. Control Fed.*, 63(2), 185–192.

Illangasekare, T. H., Armbruster, E. J., and Yates, D. N. (1995). ''Non-Agueous-Phase Fluids in Heterogeneous Aquifiers-Experimental Study.'' *J. Environ. Eng.*, 121(8), 571–579.

Newell, C. J., McLeod, R. K., and Gonzales, J. R. (1996). ''BIOSCREEN: Natural attenuation decision support system. Version 1.3.'' *Rep. EPA/600/R-96/087*, U.S. Environmental Protection Agency.

Perry, R. H., and Chilton, C. H. (1973). *Chemical Engineers' Handbook*, 5th Ed. McGraw-Hill, New York.

Rafai, H. S., Newell, C. J., Gonzales, J. R., Dendrou, S., Dendrou, B., Kennedy, L., and Wilson, J. T. (1998). ''BIOPLUME III natural attenuation decision support system: Version 1.0.'' *Rep. EPA/600/R-98/010*, U.S. Environmental Protection Agency, Washington D.C.

Rittmann, B. E. (1982). ''The effect of shear stress on biofilm loss rate.'' *Biotechnol. Bioeng.*, 24, 501–506.

Rittmann, B. E. (1993). ''The significance of biofilms in porous media.'' *Water Resour. Res.*, 29(7), 2195–2202.

Sharp, R. R., Cunningham, A. B., Komlos, J., and Billmayer, J. (1999). ''Observation of thick biofilm accumulation and structure in porous media and corresponding hydrodynamic and mass transfer effects.'' *Water Sci. Technol.*, 39(7), 195–201.

Taylor, S. W., and Jaffe, P. R. (1990a). ''Biofilm growth and the related changes in the physical properties of a porous medium. 1. Experimental investigation.'' *Water Resour. Res.*, 26(9), 2153–2159.

Taylor, S. W., and Jaffe, P. R. (1990b). ''Biofilm growth and the related changes in the physical properties of a porous medium. 2. Permeability.'' *Water Resour. Res.*, 26(9), 2161–2170.

Taylor, S. W., and Jaffe, P. R. (1990c). ''Biofilm growth and the related changes in the physical properties of a porous medium. 3. Dispersivity and model verification.'' *Water Resour. Res.*, 26(9), 2171–2180.

Torbati, H. M., Raiders, R. A., Donaldson, E. C., McInerney, M. J., Jenneman, G. E., and Knapp, R. M. (1986). ''Biofilm accumulation in sandstone.'' *J. Ind. Microbiol.*, 1, 227–234.

Vandevivere, P., and Baveye, P. (1992). ''Saturated hydraulic conductivity reduction caused by aerobic bacteria in sand columns.'' *Soil Sci. Soc. Am. J.*, 56(1), 1–13.